engineering proceedings

MDPI

Proceeding Paper

Room Temperature Electrical Analysis of Pr^{3+} Doped Silicate Glasses for Energy Storage Applications †

Gracie. P. Jeyakumar, Yasmin Jamil and Geetha Deivasigamani *

Department of Applied Sciences and Humanities, MIT Campus, Anna University, Chennai, Tamilnadu, India; email1@email.com (G.P.J.); email2@email.com (Y.J.)

* Correspondence: geetha@mitindia.edu

† Presented at the 4th International Electronic Conference on Applied Sciences, 27 October–10 November 2023; Available online: https://asec2023.sciforum.net/.

Abstract: Composite glasses possessing amorphous nature and high dielectric constants exhibit properties suitable for optoelectronic and electrochemical applications. Multi-component silica calcium phosphate glasses doped with 0.5 and 1 mol% of trivalent praseodymium (Pr^{3+}) were synthesized by the sol-gel method. The Pr^{3+} doped and undoped glasses were compared at room temperature (300 K) for analyzing their electrical variations. Dielectric studies predicted an increase in the dielectric constant and conductivity in the doped samples when compared to the undoped glass. A high dielectric constant of 89.2 was observed in the optimally doped glass at 1 kHz. The value of the capacitance increases to the order of nanofarads as the concentration of Pr^{3+} increases, indicating enhanced storage in the material. The AC conductivity of the highly doped sample evidenced a high value of 2.9×10^{-5} S/cm at 10 MHz. The Cole-Cole plot of the glasses demonstrated a single flattened semicircle due to the lack of grains. The equivalent circuitry constitutes a constant phase element (CPE) in series to a parallel circuit of a resistor and CPE. The behavior is indicative of the suitability of the glasses as cathodes. The increase of capacitance with doping in the low-frequency region suggests the use of glasses as energy storage dielectric materials in condensers.

Keywords: composite glasses; praseodymium; dielectric; Cole-Cole plot; energy storage

1. Introduction

The demand for sustainable energy grows alongside the development of substitute materials with higher efficiency for energy storage devices [1]. Crystalline electrodes that require higher annealing temperatures, resulting in unfavorable contact impurities could be replaced with glass materials, augmenting electrode-electrolyte interfacial contact and ionic conductivity levels [2]. The multi-functionality of glasses has also been extended in electrochemical industries as electrochemical sensors and batteries [3]. Silica phosphate glasses are favored in electrochemical sectors as electrodes in solid-state batteries [4], due to enhanced polymerization by the non-bridging oxygen units of the silicate and phosphate tetrahedra. Faster ionic conduction in glass electrodes and solid electrolytes by overcoming the impediment due to grain boundaries could be achieved by the use of glass modifiers [4]. Electrical studies of glass matrices with rare earth dopants, for electrochemical applications have been recently reported [5]. However, Pr^{3+} doped silica calcium phosphate glasses for low-loss energy sector applications are yet to be explored in detail.

The present article reports the analysis of the electrical properties of the Pr^{3+} doped silica calcium phosphate multi-component glasses. The findings would confirm the suitability of the glasses with high dielectric constants and increasing condenser values for inter-layer dielectric substrates. The impedance plots would suggest the potentiality of the glasses as cathode materials.

Citation: Jeyakumar, G.P.; Jamil, Y.; Deivasigamani, G. Room Temperature Electrical Analysis of Pr^{3+} Doped Silicate Glasses for Energy Storage Applications. *Eng. Proc.* **2023**, *52*, x. https://doi.org/10.3390/xxxxx

Academic Editor(s): Name

Published: date

2. Materials and Methods

The glasses were synthesized as per the scheme reported [6]. The raw materials of tetra ethoxy orthosilicate, triethyl phosphate, calcium nitrate tetrahydrate, and praseodymium nitrate hexahydrate were stirred vigorously for 2 h and left for gelation and aging for the formation of glass monoliths. The glasses were then annealed at 750 °C before being ground into powders for characterization. The glasses with 0, 0.5 and 1 mol% of Pr^{3+} are coded 0P, 0.5P and 1P respectively.

The powered glasses were pelletized and subjected to broadband dielectric spectroscopy for electrical analysis using NOVOCONTROL Technologies GmbH & Co. Germany, Concept 80 in the frequency range 100 Hz to 10 MHz at room temperature of 300 K.

3. Results and Discussion

3.1. Dielectric Studies

The complex dielectric parameter of a material is expressed by the equation,

$$\epsilon = \epsilon' + j\,\epsilon'' \quad (1)$$

The dielectric constant, ϵ' represents the energy storage capacity due to polarization on the application of electric field, while the loss factor ϵ'' represents energy dissipation. The dissipation loss could also be due to damping resistance, which prevents the orientation of dipoles with the applied electric field [7]. Figure 1 shows the variation of the dielectric constant and dissipation factor as a function of log f for all concentrations of Pr^{3+}.

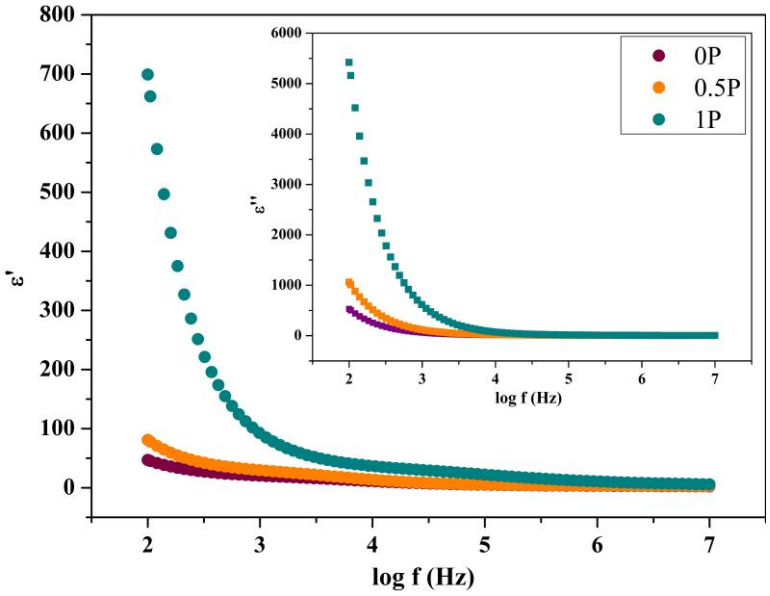

Figure 1. Variation of dielectric constant (Inset) Variation of dissipation loss as a function of frequency.

The onset of a larger dielectric constant at low frequencies is due to electrode polarization in the sample [8]. The effect increases with doping up to 1 kHz, after which the decrease is constant and independent of dopant concentration. This is because, with increasing frequencies, the total polarization in the sample lags behind the rapidly changing alternating electric fields [9]. As the concentration of the dopant increases the bonds become extensive by the non-bridging oxygens held through the Pr^{3+} ions. This could be ascribed to the increase of electrode polarization at lower frequencies and the effect becoming more pronounced with higher levels of doping [5].

3.2. Electrical Conductivity Studies

The variation of real and imaginary components of electrical conductivity versus log f is shown in Figure 2 and the inset shows the Jonscher's power law fit for conductivity in all the synthesized glasses. The increase in conductivity above the threshold frequency (hopping frequency, ω_p), and the related dielectric factors were estimated for each glass at 300 K and are given in Table 1, which are in close agreement with the values reported [10]. Below the threshold frequency, the conductivity is independent of frequency, representing minimal DC conductivity, which is demonstrated by a plateau in the graph. With an increase of Pr^{3+} concentration, ω_p shifts towards higher frequency ranges. Low conducting property at smaller frequencies is indicative of scattering; however, an increase in the conductivity value was noticed upon doping. This is due to the enhanced hopping mechanism, leading to structural variations with the addition of Pr^{3+} ions [5]. The exponent term (s), obtained from the slope of the inset which determines the magnitude of conductivity is a measure of the ionic interaction with the host matrix [11]. The pronounced AC conductivity in frequencies higher than the order of 10^5 Hz, showing dispersion could be due to the predominant influence of the electronic order of charge carriers with relatively lighter mass. This is indicative of dielectric relaxation. In the higher frequency domain, the ionic motion becomes suppressed due to the larger masses of ions and the corresponding inability to change in tune with rapidly changing electric fields.

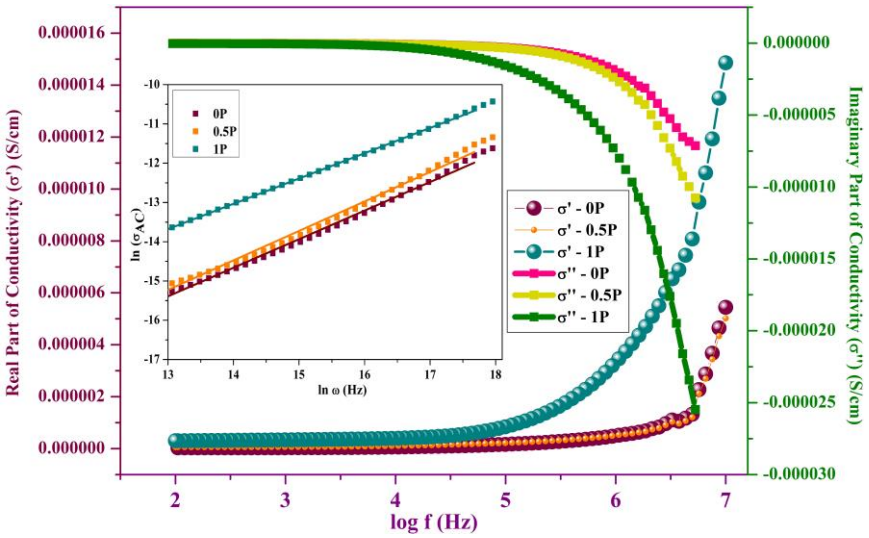

Figure 2. Variation of electrical conductivity as a function of frequency (Inset) Power law fit.

Table 1. Dielectric parameters.

Parameters/ Sample Code	Hopping Frequency ω_p (kHz)	Frequency Exponent (s)	ϵ' (at 1 kHz)	σ_{AC} (x 10^{-5} S/cm) at 10^7 Hz	Bulk Resistance (MΩ)	σ_{DC} (x10^{-6} S/cm)
0P	0.70	0.7828	18.506	0.905	2.659	0.0283
0.5P	1.03	0.7409	30.202	1.18	1.311	0.0575
1P	2.25	0.6351	89.160	2.91	0.239	0.3161

The variation of capacitance of the glasses as a function of frequency is shown in Figure 3. The capacitance of the doped and undoped glasses is negligible at higher frequencies [12]. However, in the low-frequency region dominated by electrode polarization, the capacitance increases from the order of picofarads for the sample coded 0P to the order of nanofarads corresponding to the samples 0.5P and 1P. The exponential increase of capacitance for the highly doped concentration of 1 mol% in the glasses shows that the material could be used for energy storage, sensor applications, and filter circuits in the frequency range up to 10^3 Hz.

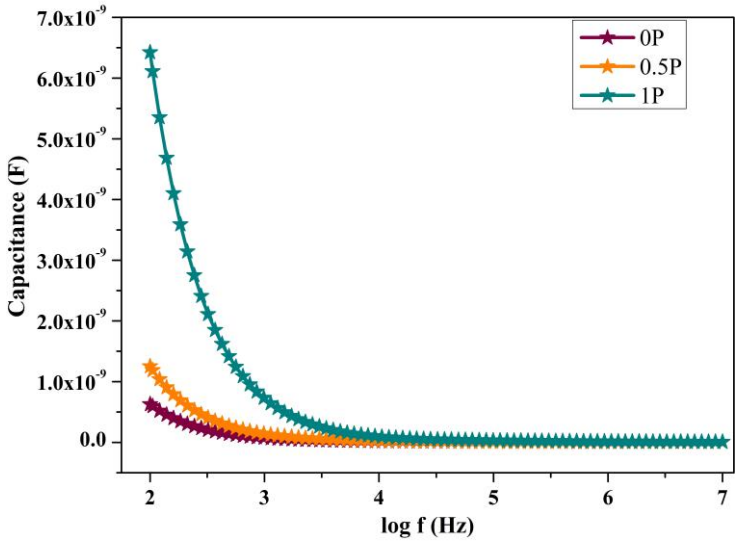

Figure 3. Variation of capacitance as a function of frequency.

3.3. Impedance Studies

Nyquist plots for all the samples are presented in Figure 4. The single depressed semicircle deduced from the Nyquist plot indicates lack of lattice symmetry, defects and inhomogeneities in the amorphous glasses [13,14]. The semicircle observed could be attributed to the effect of localized grains in the glass matrix. The center of semicircles positioned below the real impedance axis could be fitted to an equivalent circuit with a constant phase element (CPE) in series with a parallel combination of resistor and CPE and are shown in the inset of Figure 4. The depressed semicircle also validates the non-Debye relaxation mechanism of dielectric polarization in the samples [13]. It could be observed that the radius of the semicircles decreases with increasing concentrations of Pr^{3+}, indicating a decrease in bulk resistance, and subsequent increase in conductivity in the samples [13]. The DC conductivity values observed are in the order of μS/cm [12] and is found to increase with doping.

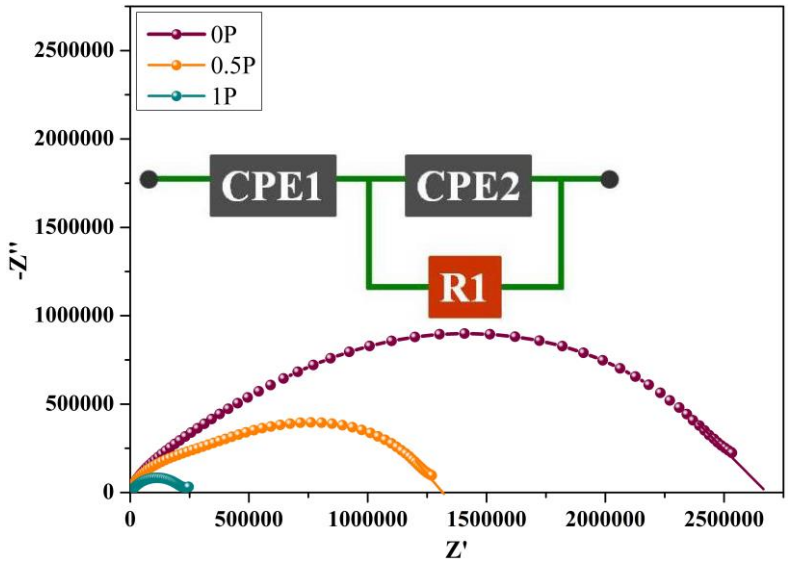

Figure 4. Nyquist plots (Inset) Equivalent circuit fitted for the glasses.

4. Conclusions

Ceramic-attributed calcium phosphate is blended with vitreous silica to selectively forge an amorphous composite glass system while doping with different concentrations

of Pr^{3+} by the sol-gel route. The increasing dielectric constant with doping substantiates the insulating behavior of the synthesized materials. At higher frequencies, enhancement of AC conductivity could be ascribed to the hopping mechanism, with a value of 2.91 × 10^{-5} S/cm at 10 MHz. Nyquist plots with a single asymmetric semicircle predicts a non-Debye model of relaxation, and represents an equivalent circuitry comprising of a resistor and constant phase elements. Electrode polarization dominant at low frequencies, contributing to the augmented capacitive values of the order of nano farads, is indicative of a proportional increment in energy storage. The composite material finds promising applications in the micro-component radio frequency capacitors. The capacitors could also be proved to be ideal for their use as filters, tuning devices, Q circuits, glass antennas, and sensor applications.

Author Contributions: Conceptualization, methodology, software, and validation, G.P.J., Y.J. and G.D.; formal analysis, and investigation, G.P.J. and G.D.; writing—original draft preparation, writing—review and editing, G.P.J. and Y.J.; visualization, G.D.; supervision, G.D. All authors have read and agreed to the published version of the manuscript.

Funding: Not applicable.

Institutional Review Board Statement: Not applicable.

Informed Consent Statement: Not applicable.

Data Availability Statement: Data is contained within the article.

Conflicts of Interest: The authors declare no conflict of interest.

References

1. Gandi, S.; Vaddadi, V.S.C.S.; Panda, S.S.S.; Goona, N.K.; Parne, S.R.; Lakavat, M.; Bhaumik, A. Recent progress in the development of glass and glass-ceramic cathode/solid electrolyte materials for next-generation high capacity all-solid-state sodium-ion batteries: A review. *J. Power Sources* **2022**, *521*, 230930. https://doi.org/10.1016/j.jpowsour.2021.230930.
2. Nagao, K.; Shigeno, M.; Inoue, A.; Deguchi, M.; Kowada, H.; Hotehama, C.; Sakuda, A.; Tatsumisago, M.; Hayashi, A. Lithium-ion conductivity and crystallization temperature of multicomponent oxide glass electrolytes. *J. Non-Cryst. Solids X* **2022**, *14*, 100089. https://doi.org/10.1016/j.nocx.2022.100089.
3. Prasad, V.; Pavić, L.; Moguš-Milanković, A.; Reddy, A.S.S.; Gandhi, Y.; Kumar, V.R.; Raju, G.N.; Veeraiah, N. Influence of silver ion concentration on dielectric characteristics of Li2O-Nb2O5-P2O5 glasses. *J. Alloys Compd.* **2019**, *773*, 654–665. https://doi.org/10.1016/j.jallcom.2018.09.161.
4. Rathan, S.V.; Govindaraj, G. Thermal and electrical relaxation studies in Li(4+x)TixNb1−xP3O12 ($0.0 \le x \le 1.0$) phosphate glasses. *Solid State Sci.* **2010**, *12*, 730–735. https://doi.org/10.1016/j.solidstatesciences.2010.02.030.
5. Prabhu, N.S.; Vighnesh, K.; Bhardwaj, S.; Awasthi, A.; Lakshminarayana, G.; Kamath, S.D. Correlative exploration of structural and dielectric properties with Er2O3 addition in BaO–ZnO–LiF–B2O3 glasses. *J. Alloys Compd.* **2020**, *832*, 154996. https://doi.org/10.1016/j.jallcom.2020.154996.
6. Gracie, P.J.; Geetha, D.; Battisha, I.K. Multifunctional praseodymium-doped composite silica glasses for UV shielding and photonic applications. *J. Phys. Appl. Phys.* **2023**, *56*, 195301. https://doi.org/10.1088/1361-6463/acc25a.
7. Ibrahim, A.M.; Badr, A.M.; Elshaikh, H.A.; Mostafa, A.G.; Elbashar, Y.H. Effect of CuO-addition on the Dielectric Parameters of Sodium Zinc Phosphate Glasses. *Silicon* **2018**, *10*, 1265–1274. https://doi.org/10.1007/s12633-017-9599-9.
8. Punia, R.; Dahiya, S.; Murugavel, S.; Kishore, N.; Tandon, R. Understanding the electrode polarization in bismuth zinc vanadate semiconducting glasses from dielectric spectroscopy: A new insight on electrode polarization effect. *J. Non-Cryst. Solids* **2021**, *574*, 121174. https://doi.org/10.1016/j.jnoncrysol.2021.121174.
9. Devaraja, C.; Gowda, G.V.J.; Eraiah, B.; Talwar, A.M.; Dahshan, A.; Nazrin, S. Structural, conductivity and dielectric properties of europium trioxide doped lead boro-tellurite glasses. *J. Alloys Compd.* **2022**, *898*, 162967. https://doi.org/10.1016/j.jallcom.2021.162967.
10. Gracie, P.; Geetha, D. Nano cristobalite embedded Er3+ doped multi-functional silica phosphate composite glasses for optoelectronic applications. *Ceram. Int.* **2023**, *49*, 25848–25867. https://doi.org/10.1016/j.ceramint.2023.05.132.
11. Barde, R.; Nemade, K.; Waghuley, S. Impedance spectroscopy study of the AC conductivity of sodium superoxide nanoparticles doped vanadate based glasses. *Mater. Sci. Energy Technol.* **2021**, *4*, 202–207. https://doi.org/10.1016/j.mset.2021.06.004.
12. Monisha, M.; Prabhu, N.S.; D'Souza, A.N.; Bharadwaj, S.; Chowdary, R.; Sayyed, M.; Alhuthali, A.M.; Al-Hadeethi, Y.; Kamath, S.D. Structural, dielectric, optical and photoluminescence studies of Tm3+ doped B2O3-BaO-MgO-Li2O-Na2O-LiF glasses featuring strong blue emission. *J. Non-Cryst. Solids* **2021**, *560*, 120733. https://doi.org/10.1016/j.jnoncrysol.2021.120733.
13. Malik, M.; Dagar, S.; Hooda, A.; Agarwal, A.; Khasa, S. Effect of magnetic ion, Fe3+ on the structural and dielectric properties of Oxychloro Bismuth Borate Glasses. *Solid State Sci.* **2020**, *110*, 106491. https://doi.org/10.1016/j.solidstatesciences.2020.106491.

14. Hanumantharaju, N.; Nayaka, R.; Nagendra, K.; Gowda, V.V.; Jayasheelan, A.; Pasha, K.S. Li2SO4 doped Li2O + B2O3 glasses: Hopping mechanism, relaxation phenomena and conductivity behavior. *Mater. Today Proc.* **2023**. https://doi.org/10.1016/j.matpr.2023.05.026.